

vein orebodies exposed over an area of dozens of square kilometers and extending for more than one kilometer updip.

6.2.4. Conclusions

The models discussed above led us to the following main conclusions.

(1) A structure of the model and simulation techniques were developed to model processes that produce vein base-metal ore mineralization because of a temperature decrease from the metal mobilization zone in granite to the region where orebodies develop in the granite.

(2) The development of mineralized veins without redeposition is the main mechanism generating ore mineralization with a subordinate role played by intraore metasomatic processes (which, nevertheless, are widespread at the deposits).

(3) Mineral stages can be caused by the evolution of a single source of ore material (which is, in our models, a zone of loosened rocks at the junction between a regional fault and its splay shear and detachment fractures), in which interactions in the rock–water system and their evolution with time played a decisive role.

(4) Equilibrium–dynamic modeling makes it possible to reproduce not only the principal structural features of the vein orebodies and the main regularities in the distributions of elements in them but also to obtain results that with high accuracy reproduce the quantitative and qualitative characteristics of natural mineral assemblages.

6.3. Models for the Development of Aureoles

Models for the development of quartz veins with base-metal ore mineralization remain incomplete until they involve processes leading to the origin of wall-rock aureoles of the distribution and redistribution of metals. The geochemical part of our research demonstrates that vein orebodies at the deposits are surrounded by infiltration-controlled aureoles of ore elements. These aureoles can be subdivided into three types: aureoles of deposition, redeposition, and leaching (see Chapter 5). We conducted a thermodynamic analysis of the processes generating these aureoles. Deposition–redeposition aureoles are the final element in the sequence mobilization zone → vein → aureole of our models. Conversely, mobilization aureoles (which were discussed above) are the first element of the sequence, as a result of which we begin our analysis of all physicochemical events.

6.3.1. Simulation methods and conditions

Simulation techniques applicable to deposition–redeposition and leaching aureoles are different and thus will be described separately.

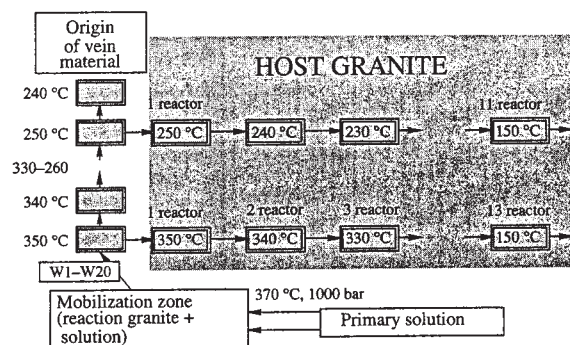


Fig. 79. Modeling scheme and model structures for the zone where deposition–redeposition aureoles develop. *W* are portions (waves) of solution from the mobilization zone; they are analogous to *NF* in Section 6.1.

Deposition–redeposition aureoles. The model of an aureole in the simulations is represented by 11–13 consecutive flow-through reactors (Fig. 79).

The number of reactors and the temperature distribution between them are determined by the initial temperature, step of temperature changes, and the assumed final temperature.

The generalized scheme of simulation is fairly simple (Fig. 79). The solution from the mobilization zone enters into a fracture conduit, in which the solution precipitates (or does not precipitate) vein minerals. Simultaneously (or subsequently), some mass of the solution that was in equilibrium with the vein material can penetrate into (filter through) the wall rocks (granite). This solution reacts with the wall rocks in the first reactor. The solution equilibrated with the rock in reactor 1 flows to reactor 2 and so on up to the last reactor in question. The transformation of the solution that leaves the last reactor is usually not considered.

Hence, the models of aureoles of this type are rigidly related (in terms of *T*, *P*, and the composition of the solutions) to the models for the development of vein bodies, and we calculate the whole succession of interaction in the solution–rock system starting from the mobilization zone, through the vein, and to the aureole. The overall number of reactors varies. For example, if the simulated aureole has an initial temperature of 350 °C, the sequence of calculations is as follows: mobilization zone (370 °C)—one reactor, zone of vein development (350 °C)—one reactor, zone of aureole development (350–150 °C)—13 reactors, i.e., 15 sequential flow-through reactors. If the simulated aureole has an initial temperature of 250 °C, the sequence of calculations is different: mobilization zone (370 °C)—one reactor, zone of vein development (350–250 °C)—11 reactors, zone of aureole development (250–150 °C)—11 reactors i.e., 23 sequential flow-through reactors (see Fig. 79). The succession of reactors is passed by 20–30 sequential portions (waves) of solutions from the mobilization zone.

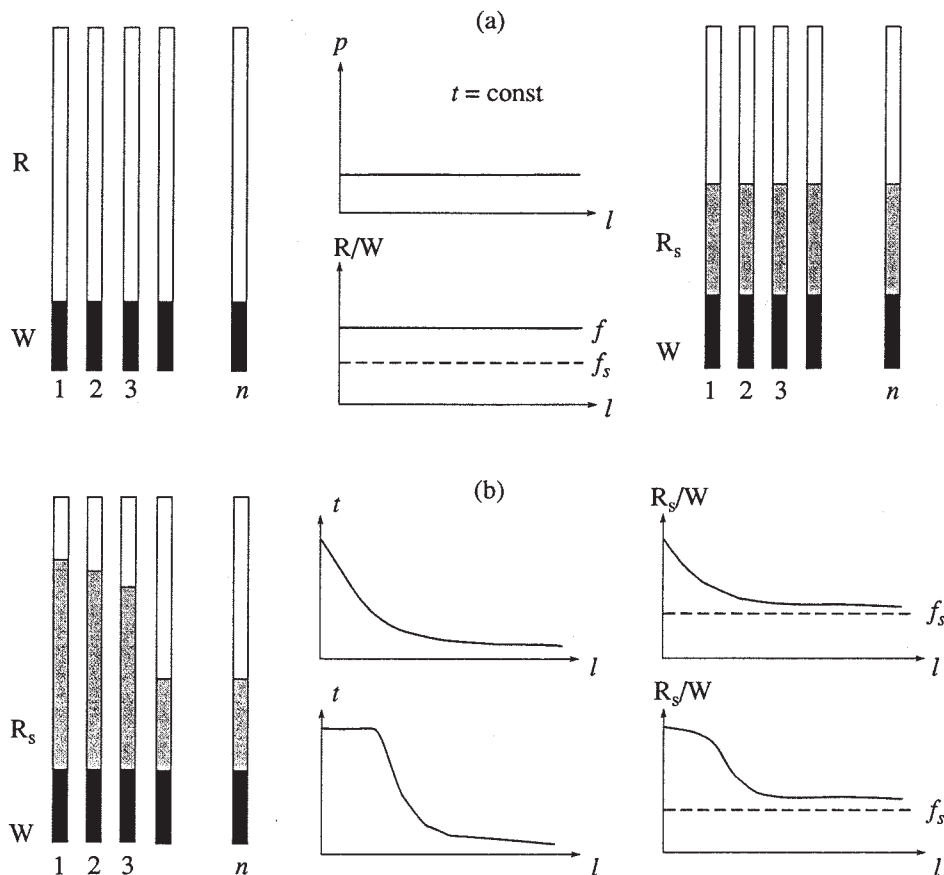


Fig. 80. Scheme showing R/W variations at a constant effective porosity of the medium (p) and a varying temperature of the country rocks. (a) At a constant temperature of the medium; (b) at a variable temperature (see text).

It was assumed in the model that the temperature in the region where the aureole develops (reactor 1) is equal to the temperature of the mineralized vein at the same topographical level. The basic (reference) models deal with three levels of aureole development: from 350, 300, and 250°C. These temperature specify the three topographical levels at which the aureole develops (the lower the temperature, the higher the aureole updip the vein). It is also assumed that conductive and convective heat transfer into the wall rocks around the fracture conduit causes a thermal heat gradient, and the temperature of the rocks systematically varies from a maximum value at a given level to the normal temperature of granite at a given depth. The constant granite temperature at the levels where veins and aureoles are formed was taken to be equal to 150°C in all calculations (as was discussed above in Chapter 5 and Sections 6.1 and 6.2). During this stage of our research, the temperature step in the gradient thermal field in the wall rocks was taken to be uniform within the nearest vicinity of the vein. For the three levels, this step was as follows:

* high-temperature level, 350–250°C (step = 10°C), 250–150°C (step = 50°C), i.e., 11 and 2 reactors;

* medium-temperature level, 300–200°C (step = 10°C), 200–150°C (step = 50°C), i.e., 11 and 1 reactors;

* low-temperature level, 250–150°C (step = 10°C), i.e., 11 reactors.

These regularities specify the temperature variations in the sequential reactors, and, correspondingly, it can be theorized that a temperature decrease is the main factor controlling the development of the aureoles. The pressure was assumed to be constant and equal to 1 kbar in all calculations. The country rock was granite from the Kholst deposit (Table 35).

A more complicated problem is the mass of rock that should be introduced into the reactors simulating the zone of aureole development. Figures 80 and 81 present the variants that demonstrate the possible character of variation correlations in the rock mass (R is whole rock mass, and R_s is the rock mass participating in the reactions) and solution (W) at different variations in the effective porosity of the granite (p includes the overall volume of the pores and of the micro- and macrofractures that can be filled with the solution) and temperature (t) over the interval (l) of the wall rocks from

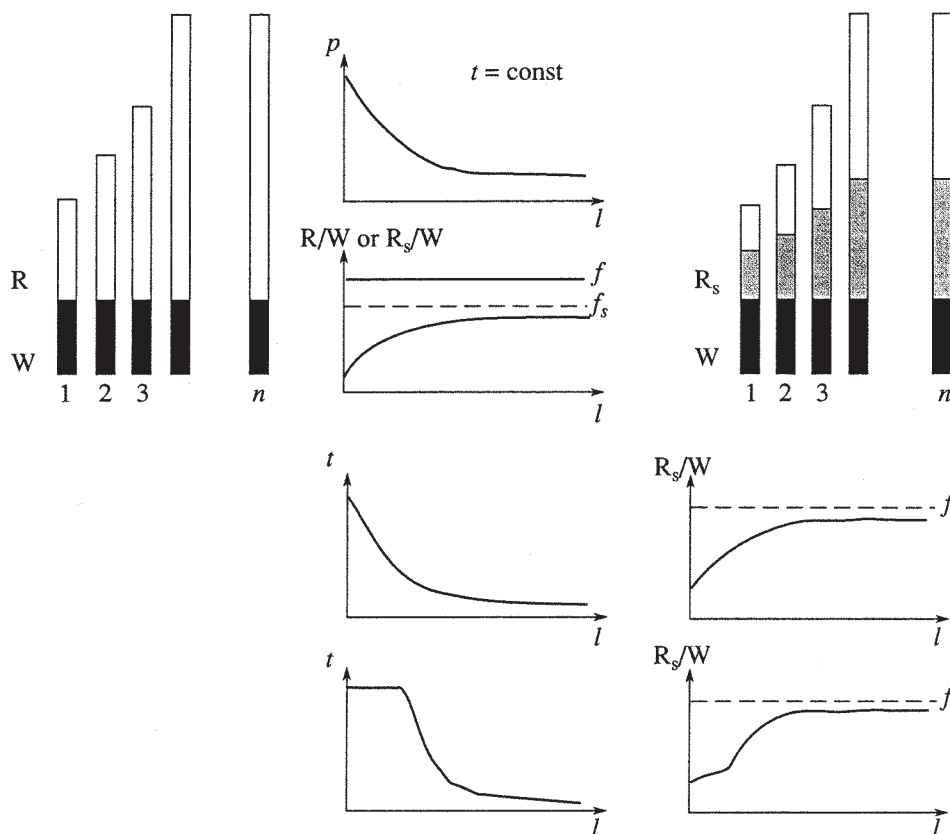


Fig. 81. Scheme showing R/W variations at a variable effective porosity of the medium (p) and a varying temperature of the country rocks (see text for explanations).

the fracture conduit to the region with a constant temperature.

Let us mentally subdivide the wall rocks into plates so that each of them could accommodate a unit mass of the solution (for simplicity, let it be 1 kg of H_2O) at a given value of p . If $t = \text{const}$ and $p = \text{const}$ throughout the whole interval l , and if the entire rock mass (R) can react with the solution, then we obtain a situation portrayed in Fig. 80a, in which $R/W = \text{const} = f$ over l . However, the more realistic situation is that in which not the entire rock mass but only part of it (R_s) can react with the solution, and, then, $R_s/W = \text{const} = f_s$ (Fig. 80a, right-hand part), with $f_s < f$.

If the wall rocks near the vein are characterized by a temperature gradient, then, at $p = \text{const}$, the reactivity of the system should vary, because the masses of rock reacting with the solution at higher temperatures are greater than those reacting at lower temperatures. Figure 80b shows two variants of temperature variations: with a high-temperature plateau (which can occur at high filtration velocities of the solution) and without it. The R_s/W ratio varies from significant values (near the fracture conduit) to lower ones (f_s). The configuration of this temperature trend is controlled by the assumed pattern of temperature changes.

However, p of the wall rocks more often decreases away from the vein because of a decrease in the number of macro- and microfractures, whose density is commonly at a maximum near the main fracture conduit. In this situation, the original scheme is modified to that portrayed in Fig. 81. If $t = \text{const}$ throughout the interval l and the entire rock mass (R) or only part of it (R_s) reacts with the solution, the situation should be that shown in the upper portion of Fig. 81, in which R/W or R_s/W gradually increase away from the fracture conduit (only the tendency is shown, although these ratios have different values, because R/W and R_s/W tend to f and f_s , respectively). If the rock near the vein has a temperature gradient, the situation is further complicated. The lower part of Fig. 81 demonstrates two scenarios of R_s/W variations at different temperatures. Both show similar tendencies in the R_s/W variations: lower values near the fracture conduit and a gradual increase to f_s away from the contact with the model vein. Obviously, the R_s/W ratio should vary within a smaller range than in a situation with $t = \text{const}$, although this is determined by the temperature values themselves (they seem to be roughly similar in the diagram).

In most of the models discussed below, we assumed that the rock mass in the reactor was constant and equal to 100 g. This was done on purpose, because we

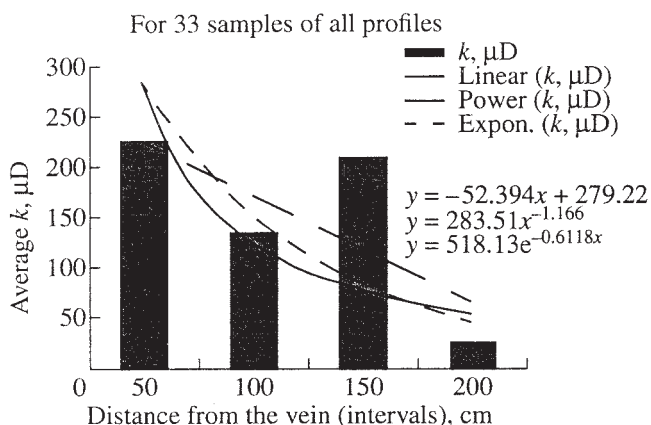


Fig. 82. Dependence of the average (over a given length) permeability value (k , μD) of the wall-rock granite on the distance from the vein (within 2 m). Equations: Linear—linear function, Power—power function, Expon—exponential function. Equations are arranged in the same order.

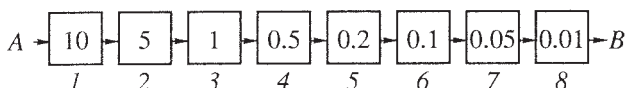


Fig. 83. Structure of the model for the genesis of a leaching aureole. A is the primary barren solution; B is the metalliferous leaching solution. Numerals in boxes (reactor contours) show the granite mass, kg; numerals outside the contours are reactor numbers. Arrows indicate the direction of the solution flow.

intended to analyze the effect of the rock–solution interaction at a minimum number of variable parameters. If other rock amounts in the reactors were used, this is indicated below where the results of certain models are discussed.

An increase in the overall permeability of rocks near a fracture conduit (see above) is known to occur in a variety of environments, and data of this kind are also available for our deposits. The permeability of rocks at the deposits was determined, in collaboration with V.M. Shmonov, by the method, and on equipment, devised at the Institute of Experimental Mineralogy, Russian Academy of Sciences [Vitovtova and Shmonov, 1982; Shmonov *et al.*, 1994, 2002]. Now we possess data on 40 samples (including their gas permeability at normal temperature) from the Kholst and Verkhni Zgid deposits [Shmonov *et al.*, 1996, 1997]. Most of these samples were taken within a 2-m interval from the fracture conduit (Fig. 82). Although data currently available are still insufficient for rigorous generalizations, even they clearly demonstrate that the permeability of the granite near the vein is prone to decrease away from vein contacts and that it strongly varies (from $n \times 10^{-18}$ to $n \times 10^{-15} \text{ m}^2$) near these contacts.

Calculations by the models of deposition–redeposition aureoles were carried out for a few combinations of conditions: polythermal and isothermal, 100 and 10 g of granite in the reactors, the rock with or without sulfide sulfur, and various compositions of the solutions.

Leaching aureoles. The modeling scheme for this type of aureoles is presented in Fig. 83.

In fact, these are somewhat modified models for the mobilization of metals from granite, which were described in detail above (Section 6.1). The primary solution at 370°C enters the system of flow-through reactors and interacts with granite that contains background concentrations of the metals. The wall-rock space is described by a succession of eight stepped reactors, whose rock masses decrease closer to the vein, because we assume that the pore fluid flow can be thickened between reactors 1 and 8. The reactors are passed by 20 successive portions (waves) of the primary solution. The calculations were conducted for an isothermal system.

6.3.2. Thermodynamic simulation results

The simulation results are subdivided into a number of groups.

1. *Reference models for deposition–redeposition aureoles ZLW1 and ZRW1* were devised based on the primary barren solution of model IS-2 (see Section 6.1). The aureoles develop near a vein that is formed in compliance with the layer (ZLW) or reaction (ZRW) mechanisms.

Modeling conditions and parameters:

* in the mobilization zone, $T = 370^\circ\text{C}$, $P = 1$ kbar, the granite mass in the reactor is 10 kg (Kholst granite), the primary solution contains $\text{H}_2\text{CO}_3 = 0.5 \text{ m}$, $\text{NaCl} = 1.0 \text{ m}$, and $\text{HCl} = 0.1 \text{ m}$;

* in the region where the filling vein is formed, $T = 350\text{--}250^\circ\text{C}$ (step = 10°C), $P = 1$ kbar, minerals precipitate from homogeneous solutions in response to a temperature decrease in models ZLW (analogously to layer model VL1, see Section 6.2) or in response to a temperature decrease and owing to reactions with vein minerals in models ZRW (analogously to reaction model VR1);

* in the zone where aureoles develop, three temperature levels are considered: 350–150°C (models ZLW1-1 and ZRW1-1), 300–150°C (models ZLW1-2 and ZRW1-2), and 250–150°C (models ZLW1-3 and ZRW1-3), the granite mass in all reactors is the same and equal to 100 g; $P = 1$ kbar.

First consider the calculation results for models ZLW1, in which veins are formed according to the *layer mechanism*.

Model ZLW1-1 simulates the development of an aureole at the lower levels of the vein (at an initial $T = 350^\circ\text{C}$).

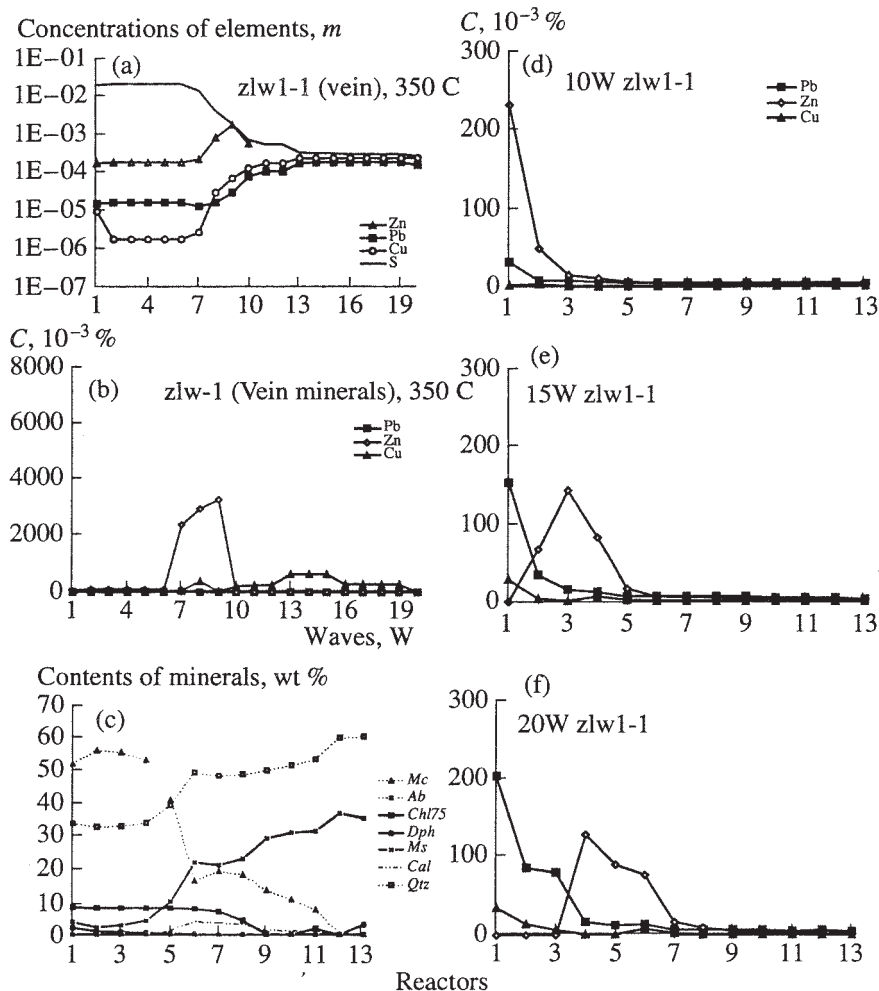


Fig. 84. Model ZLW1-1 (temperature is 350°C in the vein and 350–150°C in the aureole), Vein: (a) Zn, Pb, and Cu concentrations in the aureole-forming solution at discrete waves; (b) Zn, Pb, and Cu contents in the vein solid phases at discrete waves. Aureole: (c) main minerals of the altered country rock at wave 20; (d–f) aureole development at waves 10, 15, and 20 (temperatures in the reactors: 1—350°C, 2—340°C and so on with a step of 10°C to 11—250°C, 12—200°C, and 13—150°C). Plotted on the ordinate are wt % of elements in the solid phase.

Figure 84a shows the concentrations of solutions equilibrated with the vein mineral assemblage. These solutions come from the fracture conduit into the wall rock during each wave and produce the aureole. The regularities in the variations in the concentrations from wave to wave (portion) at a given vein segment are analogous to the variations in the mobilization zone (Fig. 51), except that the values themselves are somewhat lower because of the earlier precipitation of ore minerals in the vein. The contents of the ore elements in the vein material (i.e., the values that characterize the deposition of sphalerite, galena, and copper minerals) are demonstrated in Fig. 84b. The maximum of sphalerite deposition falls onto waves 7–9 of the leaching solution (layers 7–9), which are characterized by the highest Zn concentration.

The interaction of the solutions with rocks is associated with the deposition of sulfides of ore elements and changes in the composition of the country rock.

Figures 84d–f shows the configuration of aureoles of ore elements at three sequential “moments of time,” at waves 10, 15, and 20 of aureole development (earlier stages are characterized by the origin of very weak deposition aureoles). Obviously, changes in the proportions of ore elements in the solutions ($Zn > Pb, Cu$) are predated by the development of Zn deposition aureoles (at wave 10), which are then modified into redeposition aureoles as the Zn concentration drastically decreases in solution at waves 15–20. During the same 20 waves, Pb and Cu form only deposition aureoles. This result is quite expectable from the plots in Fig. 84a, which demonstrate that the Pb and Cu concentrations are fairly high in the solution leaving the vein at wave 20. We calculated the layer model only up to wave 20, and, thus, can only hypothesize what should be the further evolution of the aureoles. Obviously, as soon as Pb and Cu are depleted from the source (this takes place after wave 20, Fig. 51) and solutions with significantly lower

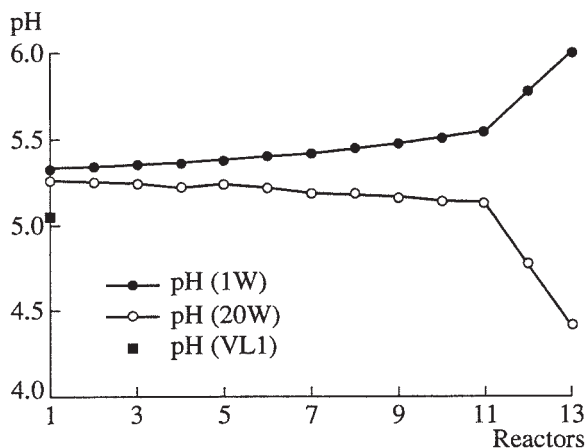


Fig. 85. Variations in the pH of the equilibrium solutions at waves 1 and 20 in model ZLW1-1 during reaction with the rock (the temperature is 350°C in the vein and 350–150°C in the aureole). Shown for comparison is the pH of the solution equilibrated with the vein minerals (model VL1) before this solution enters into reactor 1 of the aureole.

concentrations of these elements come into the interval where the aureole develops, the Pb and Zn aureoles start to change in a manner similar to that of the Zn aureole.

The precipitation of ore minerals during reactions between solutions and rocks is caused not only by the temperature decrease: sulfides also precipitate in reactor 1, in which the temperature is equal to that in the vein. Reactions with the rocks increase the alkalinity of the solution, which, in turn, shifts the reaction of sulfide dissolution toward the solid phases. The differences in pH are shown in Fig. 85.

Moreover, reactions between the solution and rock produce pyrrhotite (in amounts 0.6–2.8% at different waves) at the expense of part of the Fe and sulfide S contained in the rock. The presence of pyrrhotite main-

tains high concentrations of sulfide sulfur in the equilibrium solution (similarly to the processes in the mobilization zone, see Fig. 51), which trigger the precipitation of sulfides of ore elements.

The major-component composition of the rock is strongly modified (Fig. 84c). For example, during the final stage (wave 20), more than 50% potassic feldspar is formed in the first four reactors, along with 35% quartz, up to 5% Fe–Mg chlorite, and minor amounts of sericite, while the amount of potassic feldspar formed in reactors with low temperatures (reactors 7 through 13) sharply decreases and the sericite and quartz concentrations increase (to 40 and 50%, respectively).

Model ZLW1-2 simulates the development of an aureole at the “intermediate” levels of the vein (at a starting temperature of $T = 300^\circ\text{C}$).

The general tendencies are very similar to those of the previous model, but there are also some minor differences. The Pb concentration is higher than the Cu concentration at nearly all waves. The maximum of sphalerite deposition in the vein also falls onto waves (portions) 8–9 of the leaching solution (layers 8–9 of the vein).

As in the model at 350°C, Zn deposition aureoles are the first to develop, but no redeposition aureoles are produced and there is only a tendency toward their origin at wave 20 (Zn is partly redeposited from reactor 1 to reactors 2 and 3). Both Pb and Cu form exclusively deposition aureoles. This character of aureoles is caused by a decrease in the solubility of sulfides with decreasing temperature (Fig. 86).

Model ZLW1-3 reproduced the origin of an aureole at the “upper” levels of the vein (at a starting temperature of 250°C).

The temperature decrease results in systematic differences from the results of the two previous models. Figure 87a shows the compositions of solutions in equilibrium with the vein mineral association. The weak increase in the Pb and Cu concentrations noted in

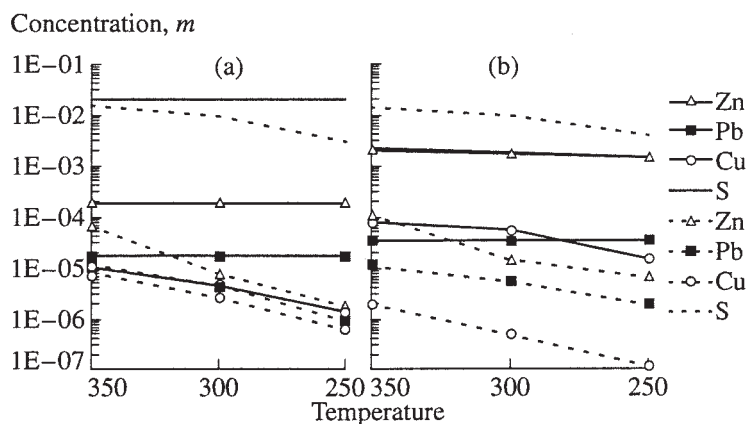


Fig. 86. Concentrations of components in the solutions at waves (a) 1 and (b) 9 in models VL1 and ZLW1. Solid lines show elements in the solution in the vein (model VL1), and dashed lines correspond to elements in reactor 1 of the aureole (model ZLW1).

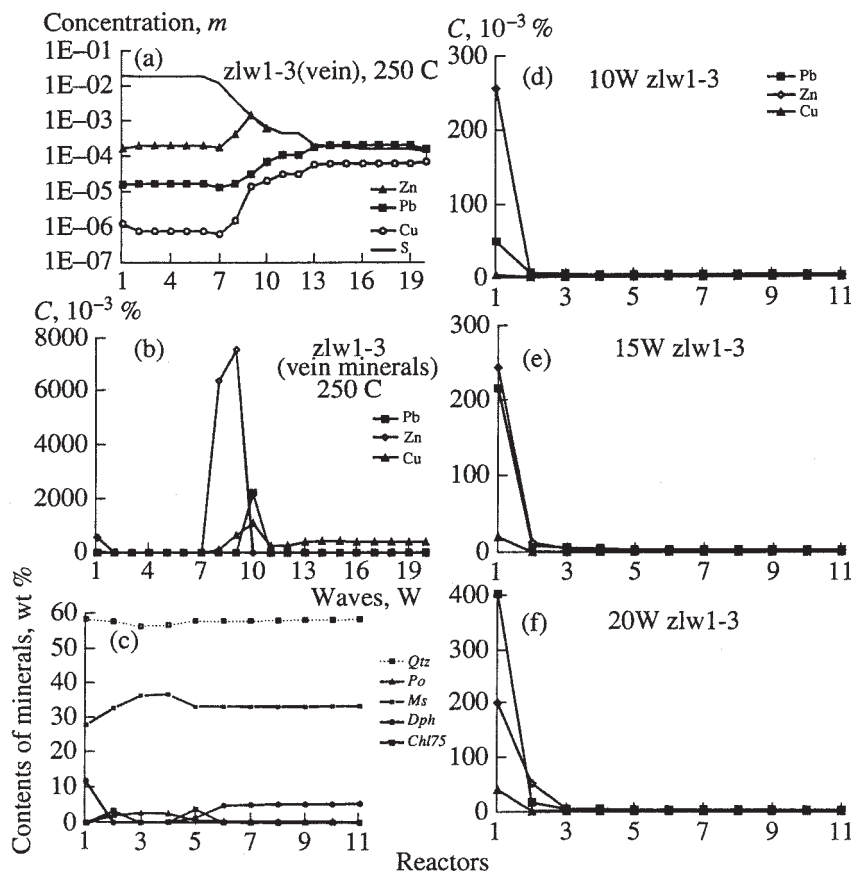


Fig. 87. Model ZLW1-3 (the temperature is 250°C in the vein and 250–150°C in the aureole). Vein: (a) Zn, Pb, and Cu concentrations in the aureole-forming solution at discrete waves; (b) Zn, Pb, and Cu contents in the vein solid phases at discrete waves. Aureole: (c) main minerals of the altered country rock at wave 20; (d–f) aureole development at waves 10, 15, and 20 (temperatures in the reactors: 1—250°C, 2—240°C, and so on, with a step of 10°C to 11—150°C). Plotted on the ordinate are wt % of elements in the solid phase.

model ZLW1-2 becomes more significant here, and the concentrations of ore elements comprise the succession $Zn > Pb > Cu$. However, the main tendencies in the variations of the concentrations of ore elements in solutions equilibrated with the vein mineral assemblages are very close to the tendencies common for all three models. The contents of ore elements in the vein are displayed in Fig. 87b. The deposition of sphalerite at this temperature attains a maximum of 8% (in layers 8–9 of the vein).

The main minerals of the altered rock (at wave 20) are shown in Fig. 87c: quartz accounts for nearly 60%, sericite comprises 30–35%, and chlorites are contained in amounts of 5–10%. The contents of these minerals hardly vary between the reactors.

Figure 87d–f shows the resulting aureoles of ore elements. Similarly to model ZLW1-2, this model clearly demonstrates that only deposition aureoles develop, and there is only a tendency of Zn redeposition at wave 20.

Now consider the results of calculations by ZRW1 models (the vein develops according to the reaction

mechanism). Although rare, veins at the deposits in question could also be formed in compliance with the reaction mechanism (as was described in Section 6.2). The results for the reaction models are easier to process; because of this they were calculated for 30 and more solution waves, which, in turn, allowed us to examine some processes that could not be studied in models ZLW1.

Model ZRW1-1 describes the development of an aureole at the “lower” levels of the vein (at a starting temperature of $T = 350^\circ\text{C}$).

All modeling conditions remain the same as in model ZLW1-1 except for two: the vein is formed by the reaction mechanism, and the processes are traced up to wave 30 of solution from the mobilization zone. The results of our simulations are presented in Fig. 88. The concentrations of the solutions in equilibrium with the vein mineral assemblage are practically identical to those in model ZLW1-1 (Fig. 84a). The solutions after wave 23 become absolutely barren. In the further analysis of the results, it should be borne in mind that the mineral composition of the vein is modified by each

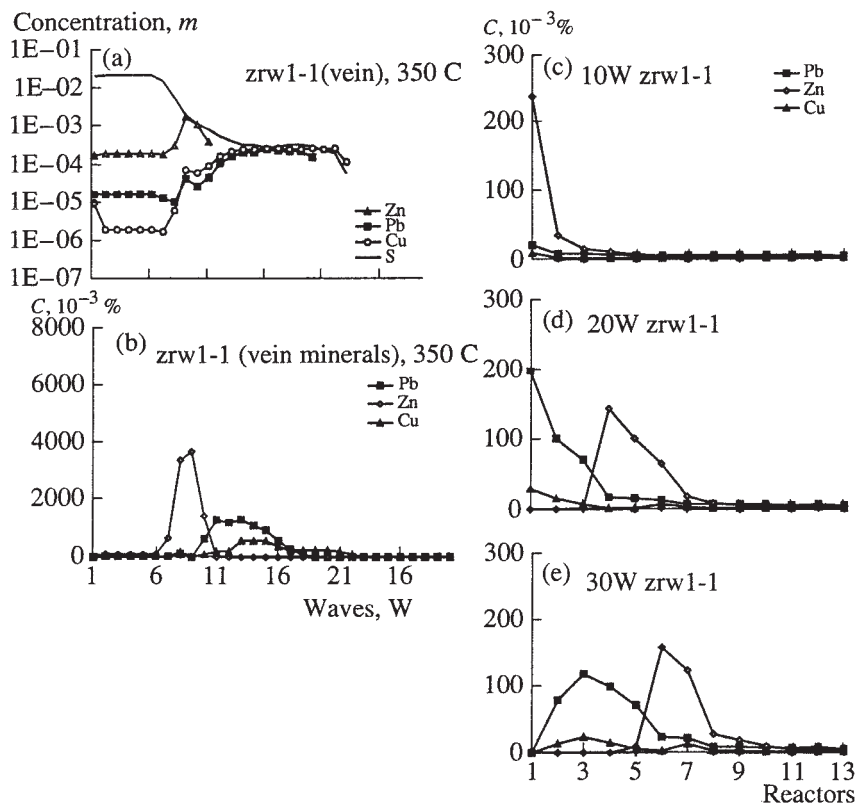


Fig. 88. Model ZRW1-1 (the temperature is 350°C in the vein and 350–150°C in the aureole). Vein: (a) Zn, Pb, and Cu concentrations in the aureole-forming solution at discrete waves; (b) Zn, Pb, and Cu contents in the vein solid phases at discrete waves. Aureole: (c–e) aureole development at waves 10, 20, and 30 (temperatures in the reactors: 1—350°C, 2—340°C, and so on, with a step of 10°C to 11—250°C, 12—200°C, 13—150°C): Plotted on the ordinate are wt % of elements in the solid phase.

wave. Correspondingly, the solution of each wave is in equilibrium only with the respective vein mineral assemblage. For example, at wave 30, the vein does not contain any ore minerals at all (Fig. 88b), and whatever was deposited by waves 7–20 is dissolved and transported to low temperature levels by later solution portions (waves 21–30) from the mobilization zone. Conversely, at the layer mechanism, ore minerals are preserved in earlier layers.

It is interesting to follow the transformations in the aureoles. At waves 10 and 20 (Fig. 88c–d), aureoles are analogous to those in model ZLW1-1, but later, when barren solutions (waves 24–30) start to enter the zone where the aureoles are formed, transformations affect not only the Zn aureoles but also those of Pb and Cu. This phenomenon does not manifest itself in model ZLW1-1 because the number of the waves was too small, but in this model, redeposition aureoles start to develop for all metals.

The mineral composition of the altered rocks in this model fully corresponds to that described in model ZLW1-1 (at wave 20).

Model ZRW1-2 corresponds to the development of an aureole at the intermediate levels of the vein (at a starting temperature of $T = 300^\circ\text{C}$).

All of the results obtained, except the mineral formation in the vein, are virtually identical with the results of model ZLW1-2. Late in the course of the process, a Zn redeposition aureole is formed, but Pb and Cu redeposition only begins.

Model ZRW1-3 simulates the development of an aureole at the “upper” levels of the vein (at a starting temperature of $T = 250^\circ\text{C}$).

The differences, caused by a different mechanism producing the vein, are clearly pronounced in model ZRW1-3 (Fig. 89). For example, Fig. 89a demonstrates that the solutions equilibrated with the vein minerals are characterized by a remarkable separation of the ore elements (the concentrations in the sequence Zn–Pb–Cu differ by one order of magnitude or more).

The differences in the concentrations of the solutions are reflected in the aureoles (Fig. 89c–e). For example, in model ZLW1-3, whose Pb concentrations are higher, we obtained a Pb content in the aureoles as

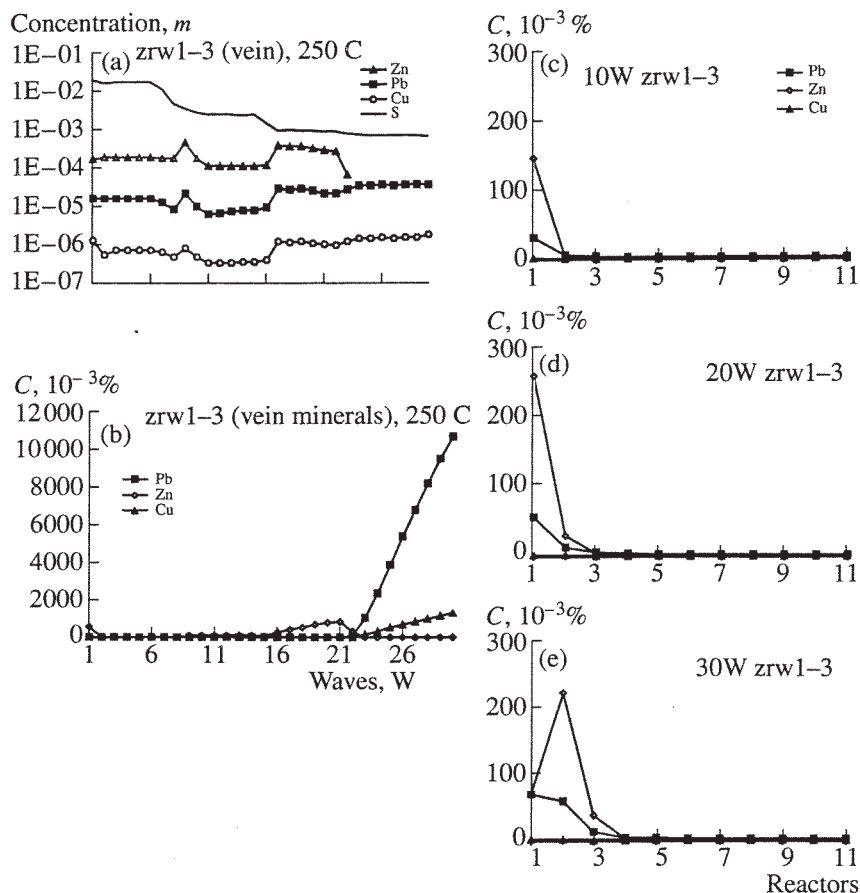


Fig. 89. Model ZRW1-3 (the temperature is 250°C in the vein and 250–150°C in the aureole). Vein: (a) Zn, Pb, and Cu concentrations in the aureole-forming solution at discrete waves; (b) Zn, Pb, and Cu contents in the vein solid phases at discrete waves. Aureole: (c–e) aureole development at waves 10, 20, and 30 (temperatures in the reactors: 1—250°C, 2—240°C, and so on, with a step of 10°C to 11—150°C). Plotted on the ordinate are wt % of elements in the solid phase.

high as 0.4%, whereas the maximum Pb concentration in the aureole of model ZRW1-3 is only 0.08%.

The final stages of the processes are marked by the origin of a Zn redeposition aureole (wave 30, Fig. 89e), but Pb redeposition only begins (Cu is contained in insignificant amounts).

The other models for the genesis of deposition–redeposition aureoles presented below are regarded as complementary. Because of this, we restricted their consideration to only one temperature (350°C) and based them on the reaction mechanism of vein genesis.

2. Model ZRW2-1 for a deposition–redeposition aureole. All modeling conditions and parameters are analogous to those in model ZRW1-1. The only difference is the mass of granite, which is equal to 10 g in each reactor. The decrease in the rock mass in reactors allowed us to elucidate the effect of the rock/water mass ratio on the characteristics of the aureoles.

The aureoles thus obtained (Fig. 90) differ from the aureoles of the basic model ZRW1-1 (Fig. 88). First, the process of aureole formation is more intense: starting from waves 10–15, the metals are actively redepos-

ited. Second, each metal forms a number of redeposition maxima in the aureole, and the rock itself is basically modified. It does not contain any newly formed potassic feldspar (Fig. 84c), but instead, bears quartz–sericite with chlorite metasomatic assemblages (Fig. 91).

The origin of the second spatial maximum of metal redeposition in the aureoles of model ZRW2-1 (in reactors 12–13) is quite simple: this is a result of a sharp decrease in the temperature. While the temperature step before reactor 11 is 10°C, the transition to reactor 12 is specified by a decrease of 50°C. Thus, the effect in question is simply an artifact. We did not trace the development of the aureole as far as this in model ZRW1-1.

However, the second maximum can form not only in the last reactors. This can be exemplified by the aureole at wave 15 (Fig. 92). The cause of this phenomenon is a change in the concentration and behavior of sulfur in the system (Fig. 93), as illustrated most clearly by changes in the Cu minerals: chalcocite in reactors 1–2, bornite in reactors 3–6, and chalcopyrite in reactors 7–

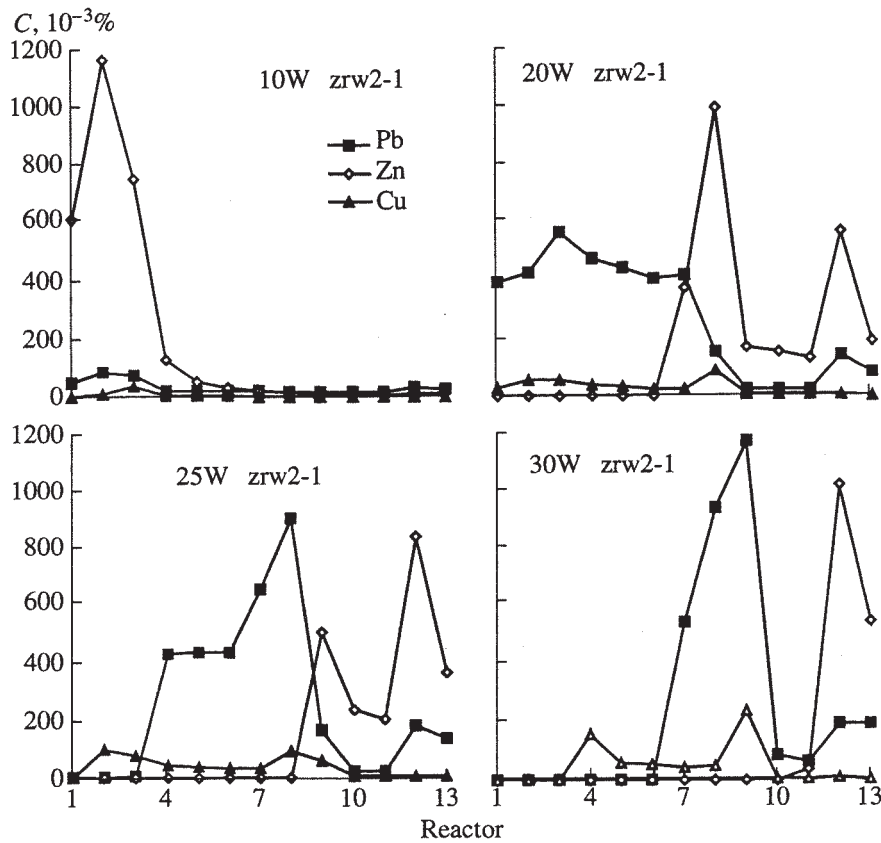


Fig. 90. Model ZRW2-1 (the temperature is 350°C in the vein and 350–150°C in the aureole). Aureole development at waves 10, 20, 25, and 30 (temperatures in the reactors: 1—350°C, 2—340°C, and so on, with a step of 10°C to 11—250, 12—200, and 13—150°C). Plotted on the ordinate are wt % of elements in the solid phase.

13 (reactors 8–13 also contain pyrite). In addition, the solutions of model ZRW2-1 have lower pH, and the differences in their acidity increases starting from the beginning of aureole development to the latest stages of this process (Fig. 94).

3. Model ZRW3-1 for a deposition–re-deposition aureole. All modeling conditions and parameters are

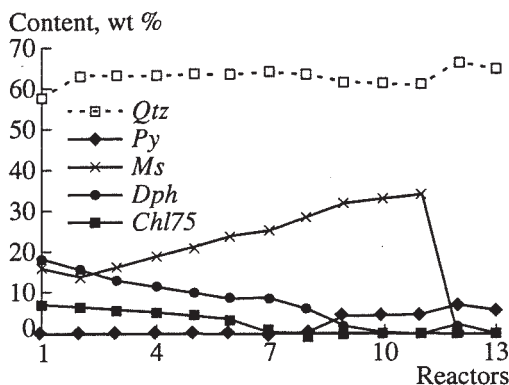


Fig. 91. Model ZRW2-1: the main minerals of the metasomatically transformed country rock at wave 20.

analogous to those assumed for model ZRW1-1 with only one exception: the granite in which the aureole develops contains no sulfide sulfur (all sulfur is brought by the solution from the mobilization zone). The simulations were aimed at determining the effect of sulfur on aureole development.

At all waves, we obtained aureoles fully identical to those in model ZRW1-1. Of course, there are minor differences in the contents of some minerals, but they are not major. It is thus reasonable to believe that the sulfur contained in the rocks in which the aureole develops does not play any significant role in the deposition of sulfides in this rock.

4. Model ZRW4-1 for a deposition–re-deposition aureole. All modeling conditions and parameters are analogous to those in model ZRW1-1. The only difference is as follows: the aureoles develop under isothermal conditions (350°C). The goal of the simulations was to clarify the effect of isothermal conditions on the development of aureoles.

The aureoles thus obtained (Fig. 95) strongly differ from the aureoles of basic model ZRW1-1 (Fig. 88). The high temperature in the zone where aureoles are generated and, consequently, the high solubility of all minerals predetermines the character of the origin and

evolution of aureoles in this model. The data presented in Fig. 95 first seem to be amazing: the occurrence of a Zn deposition aureole at wave 10, the absence of Zn in the aureole at wave 20, intense deposition of Pb in reactor 1 at wave 20, and a very low Pb concentration in the aureole at wave 30. These behaviors of the elements are caused by the very high "rates" of the development and transformation of the aureoles (which are caused by the high temperature). Ore elements "dart" through thirteen reactors and leave the region examined in the models. To explicate, we present a more detailed plot for the Zn behavior over the "time interval" corresponding to waves 10 through 15 (Fig. 96). As can be seen, the Zn aureole passes through all stages of transformations: the deposition aureole gives way to a redeposition aureole, which then starts to shift away from the fracture conduit and extends beyond reactor 13 at wave 16. The behaviors of Pb and Cu are analogous (except that they drop behind Zn).

There are characteristic differences between the alteration grades of the rock in the model with a temperature decrease from 350 to 150°C and the model with a constant temperature (Fig. 97). In the polythermal model, the K-feldspathization at high temperatures (reactors 1–5) gives way to the development of quartz-sericite assemblages at low temperatures. In the isothermal model, the zone of K-feldspar alterations in the vicinity of the vein grades to practically unaltered rocks away from the vein (in reactors 5–13). As can be seen from the models, K-feldspathization is typical of high-temperature regions near the vein and only of models with a rock mass in the reactors equal to 100 g, in contrast to models with 10 g of rock, in which quartz-sericite with chlorite assemblages are formed at the same temperature (Fig. 91).

5. *Model FM1 for leaching aureoles.* The modeling conditions and parameters are as follows (see Fig. 83 for the simulation scheme): 370°C, 1 kbar, 8 stepped flow-through reactors, granite from the Kholst deposit; rock is unequally distributed between the reactors (10 kg in reactor 1, 5 kg in 2, 1 kg in 3, 0.5 kg in 4, 0.2 kg in 5, 0.1 kg in 6, 0.05 kg in 7, and 0.01 kg in 8); the solution entering reactor 1 has a constant composition ($\text{H}_2\text{CO}_3 = 0.5 \text{ m}$, $\text{NaCl} = 1.0 \text{ m}$, $\text{HCl} = 0.1 \text{ m}$, i.e., a composition analogous to that of solution in mobilization model IS-2); the reactors are passed by a succession of 20 portions (waves) of the primary solution.

The simulated distributions of ore elements between eight reactors are shown in Fig. 98. The data are presented not in traditionally used wt % but as normalized to the background concentrations of the elements in the rocks, i.e., in the form of ratios of the metal content in each reactor to the background. This is justified, because we deal here with leaching aureoles, whose concentrations of ore elements are close to the background values.

For example, let us consider the behavior of Zn. During the initial stages (waves) of the process, Zn is

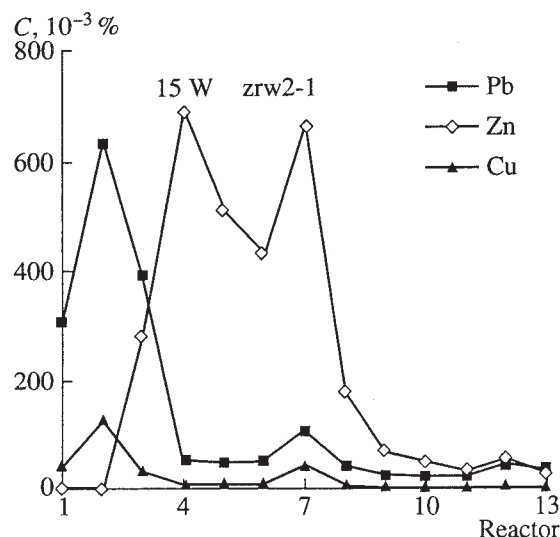


Fig. 92. Aureole development at wave 15 (model ZRW2-1). Reactor temperatures: 1—350, 2—340, and so on, with a step of 10°C to 11—250, 12—200, and 13—150°C. Plotted on the ordinate is wt % of element in the solid phase.

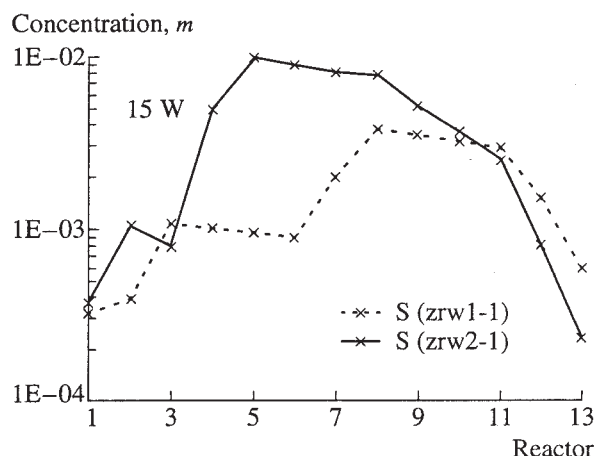


Fig. 93. Comparison between the sulfur concentrations in solutions equilibrated with the mineral assemblages in reactors of models ZRW1-1 and ZRW2-1 at wave 15.

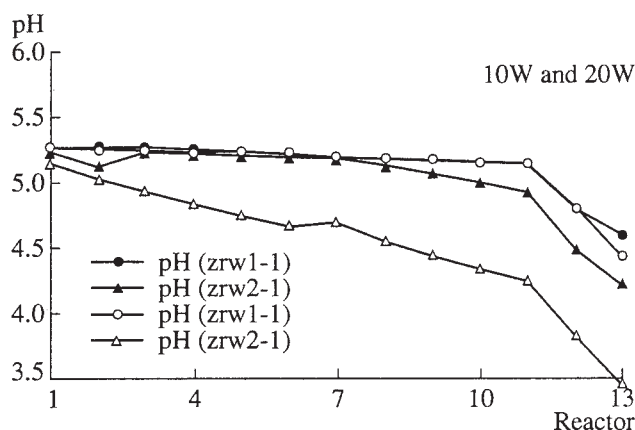


Fig. 94. Comparison between the pH of solutions equilibrated with the mineral assemblages in reactors of models ZRW1-1 and ZRW2-1 at waves 10 and 20. Solid and open symbols correspond to waves 10 and 20, respectively. The reactor temperatures vary from 350 to 150°C.

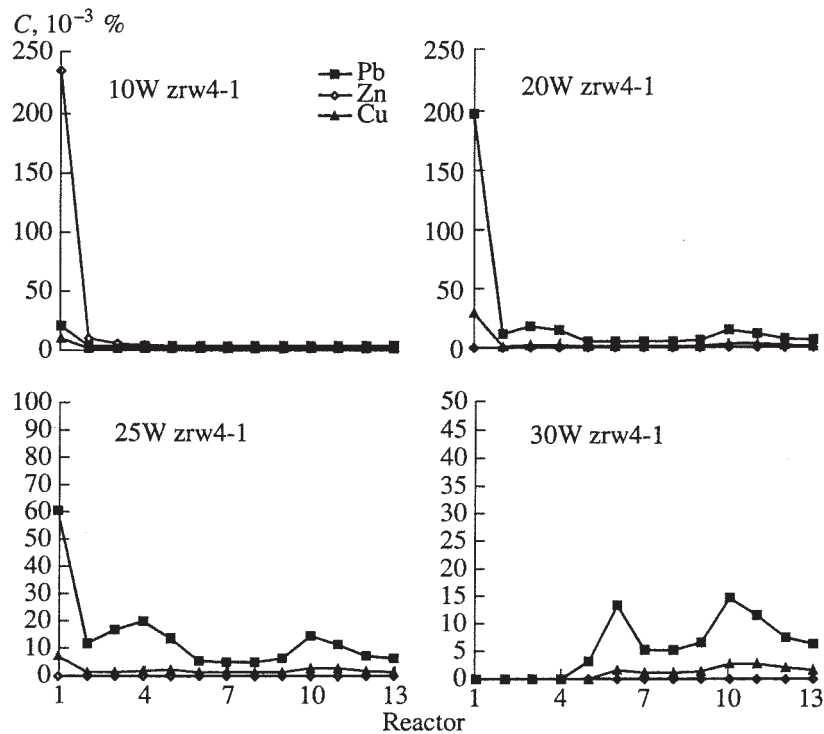


Fig. 95. Model ZRW4-1 (temperature is 350°C in the vein and aureole). Aureole development at waves 10, 20, 25, and 30. Plotted on the ordinate is wt % of element in the solid phase.

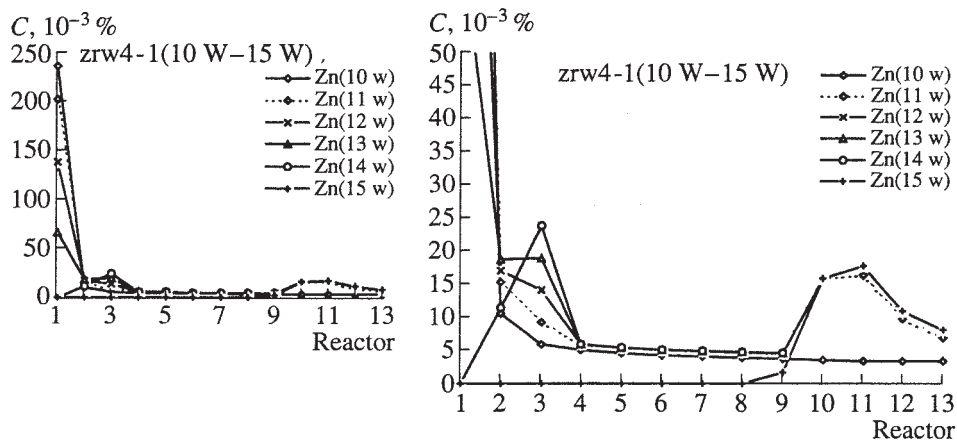


Fig. 96. Detailed plot for the development of the Zn aureole at waves 10–15 (model ZRW4-1). The maximum ordinate value in the left-hand plot is 0.25%. The right-hand plot is detailed to 0.05%.

leached from reactor 1 and redeposited in reactor 2. This is clearly seen from Fig. 98a, which portrays the situation at wave 4. The Zn distributions in other reactors correspond to the background. The Zn concentration at wave 8 is below the background in the first two reactors, more than two backgrounds in reactor 3, and 1.5 backgrounds in reactors 4–8. At wave 10, Zn is completely extracted from all eight reactors.

The behaviors of Pb and Cu are almost completely similar to that of Zn but are shifted in terms of “time” (waves). By wave 20, Pb contents above the background occur only in reactors 6–8, and Cu contents above the background are restricted to reactors 3–8. In the direction away from the vein (from reactor 8 to reactor 1), the mobility succession Zn—Pb—Cu is formed in the leaching aureoles.

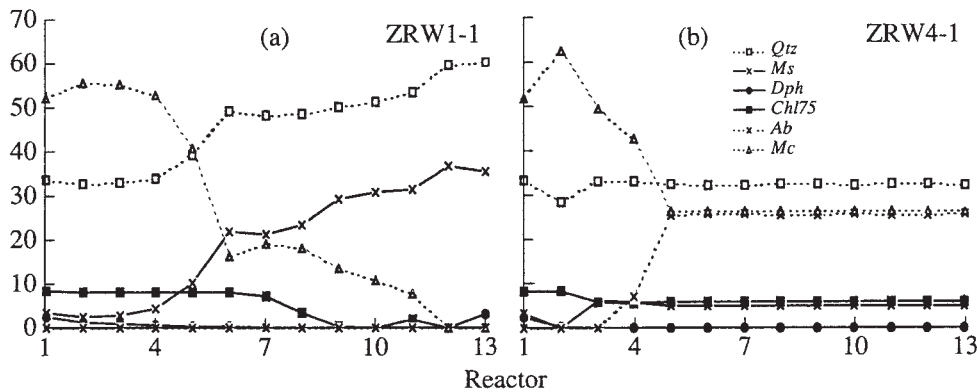


Fig. 97. Main minerals of the metasomatically altered country rock at wave 20. (a) Model ZRW1-1, (b) model ZRW4-1.

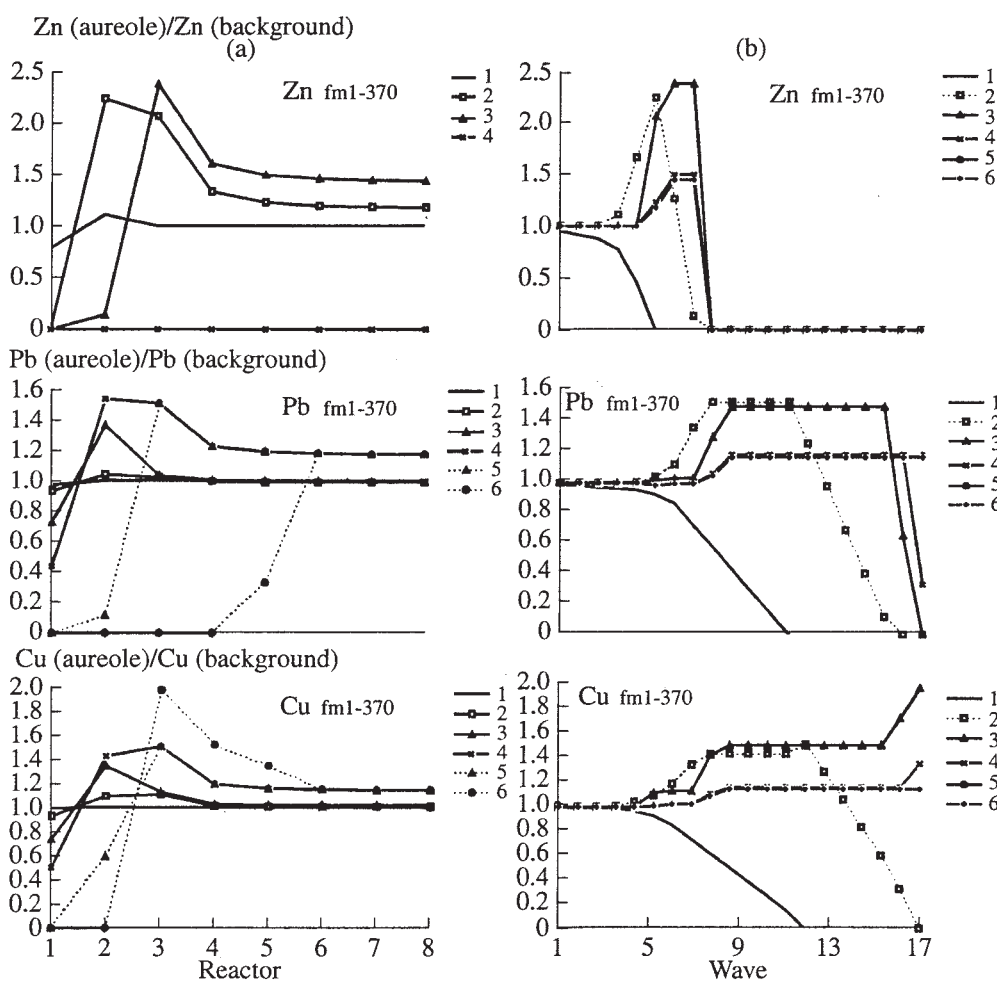


Fig. 98. Model FM1: structure of leaching aureoles. Variations in the contents of ore elements normalized to the background contents in the rock between (a) discrete reactors (symbols show different waves) and (b) discrete waves (symbols show different reactors).

Figure 98b demonstrates how elements are redistributed between the waves. For example, a Zn maximum is formed at waves 7–8 in reactor 3. No Zn remains at wave 20 in reactor 8 (before the vein), and the ratios of Pb and Cu are slightly higher than one.

The rock undergoes insignificant transformations during its reaction with the solution. The most strongly altered portion of the near-vein space is the rock in reactor 1 (Fig. 99), i.e., the rock most distant from the vein.

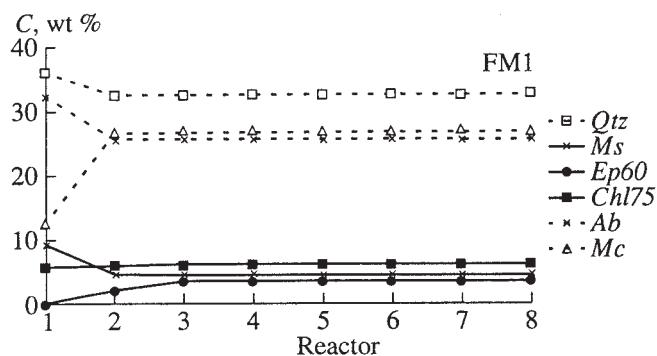


Fig. 99. Model FM1: main minerals of the metasomatically altered country rock at wave 20.

The integral effect of leaching was analyzed above (see section 6.1). This model illustrates the dynamics of the evolution of the structure of such aureoles with time.

6.3.3. Discussion of the simulation results and their comparison with natural observations

(1) Our models demonstrate that deposition and redeposition aureoles develop in the rocks hosting veins with base-metal ore mineralization.

(2) The models confirm the conclusion, which was drawn based on studying natural rocks, that the development of deposition and redeposition aureoles testifies to the asynchronous decrease in the concentrations of Zn, Pb, and Cu in the hydrothermal solution. It was established in the models that systematic variations in the composition of the hydrothermal solution up to its barren level result in an evolution of the structure of the aureole and an increase in its thickness. For example, the early stages of most models are marked by the origin of Zn, Pb, and Cu deposition aureoles, and the concentrations of the elements in them are distributed in the same succession, because the concentration of Zn is higher than that of Pb, which, in turn, is higher than the concentration of Cu. The solution becomes barren of Zn, and the earlier aureole of deposition starts to transform into a redeposition aureole. Simultaneously, Pb and Cu continue to accumulate in the deposition aureoles. The Pb concentration in the solution decreases, and a Pb redeposition aureole starts to grow in the wall rocks around the vein.

Our modeling results are consistent with the established fact of preferable Zn accumulation in natural aureoles (see Chapter 5). This is favored by three factors: the background concentration of Zn in the granite is higher than those of Pb and Cu; the solubility of sphalerite is high, as a result of which the metalliferous solution can bear high Zn concentrations; and Zn is the first to be mobilized from the source rocks and the first to be redeposited in aureoles.

(3) Our simulations demonstrate that a temperature gradient and chemical interaction in the solution–rock system are the main factors controlling the deposition of ore material in the aureole.

A temperature gradient predetermines the general structure of the developing aureole and the arrangement and configurations of individual maxima of each metal in it. Of course, this takes place when an evolving hydrothermal solution continues to enter the system. If the solution is metalliferous in terms of all components, only deposition aureoles are generated (as is the case with the early stages in our models). If the solution becomes instantaneously barren of all the components, redeposition aureoles of all of the components start to grow and the maxima of the contents of these components in the aureole start to synchronously (or nearly synchronously, depending on the differences in the solubility of the components) shift. Equal distances of Zn, Pb, and Cu maxima from the vein are very rare in natural aureoles, although these rare situations can be expectedly characterized by a drastic change in the concentrations of the metals in the solution. The compositional evolution of the metalliferous solution results in the asynchronous development of aureoles of individual ore elements and the separation of their deposition maxima in the wall rocks, which is a characteristic feature of natural aureoles.

In the models discussed above, we chose a practically linear character of the temperature decrease in the wall rocks around the vein, although this situation should be not very common in nature. The temperature usually decreases nearly exponentially, or this dependence is complicated by a high-temperature plateau near the fracture conduit (see Figs. 80 and 81). However, this should not bring about any principal differences in the generation of the aureole. The only exception is a linear scale of material deposition effects in the aureole. A linear scale was chosen in our models provisionally and is predetermined by the assumed equal masses of the rock and solution in the reactors, although it was mentioned during the discussion of the simulation techniques that the variations regularities in the rock/water ratio can be more complicated.

The role of the country rocks as an agent of ore precipitation is pronounced most clearly in the first reactors in the aureole zone of all models. In these reactors, ore material is always deposited (the temperatures in the vein and reactor 1 are equal) because of the strongly unequilibrated character of the fracture (vein-forming) solution with respect to the country rocks. Reactions in the solution–rock system modify many characteristics of the solution, including its pH (the solutions become more alkaline, as can be seen, for example, from Fig. 85), a parameter usually responsible for the deposition of ore material. The main factor controlling the development of the aureole in the next reactors is the temperature decrease.

The results of two models, ZRW1-1 and ZRW2-1, can be utilized to analyze the effect of variations in the rock/water ratio on the development of the aureole (the rock masses in each reactor are 100 and 10 g, respectively, in the former and latter models). As the rock amount in the reactors decreases, the redeposition aureoles of ore elements become more extensive and expand for greater distances from the vein (Figs. 90, 92). Conversely, the aureoles develop more sluggishly when the rock masses are greater (Fig. 88). This is caused mostly by the differences in the pH variations. Figure 94 makes it possible to compare the pH of solutions in the reactors of models ZRW1-1 and ZRW2-1 at waves 10 and 20 during the development of an aureole. The solutions of model ZRW2-1 are more acid, and the ore minerals are dissolved more actively and precipitate more quickly with a temperature decrease. The changes in the pH are a consequence of transformations in the buffer association of aluminosilicate minerals ($Qtz + Ms + Mc$ in ZRW1-1 at wave 20 in reactors 1–11 and $Qtz + Ms + Chl$ in ZRW2-1 over the same interval).

(4) Relatively intense aureoles of Zn and Pb deposition (Fig. 95) restricted to narrow zones near the vein can develop under isothermal conditions because of solution–rock interactions. However, as soon as barren solutions start to enter the zone of aureole development, these deposition aureoles are actively redeposited; their material is disseminated, forms no pronounced maxima, and is then removed to intervals far away from the fracture conduit. The whole vein vicinity thereby starts to act similarly to the mobilization zone of metals (described in much detail above), with the transformation rate of the aureoles controlled by the temperature level. The results of this model illustrate what should happen if the temperature sharply decreases after an interval with isothermal conditions. This zone should be marked by the deposition of the bulk of the ore mineralization and the development of intense content maxima. If the temperature decreases over a narrow spatial interval, it is reasonable to expect that all ore elements should form redeposition maxima at equal distances from the vein, regardless of the compositional evolution of the mineralized metalliferous solution (over the narrow interval where the temperature decreases, the maxima of metal contents will, of course, be separated but should occur at nearly equal distances from the vein). This is another variant explaining the possibility of the spatial combination of redeposition maxima of ore elements.

Isothermal aureoles of ore elements are similar to leaching aureoles, but the wall rocks of veins are strongly altered in the former (Fig. 97 and others) and remain practically unaltered in the latter aureoles (Fig. 99).

(5) Our geochemical investigations demonstrate that Zn normally predominates in the aureoles, while Zn predominance over Pb or Pb over Zn are equally probable in the veins (see Chapter 5, Fig. 45). Our mod-

els explain how these situations can be implemented. For example, in model ZRW1-3 (Fig. 89), Pb predominates in the vein ($Pb > Cu \gg Zn$), but Zn predominates in the aureole ($Zn > Pb \gg Cu$). Examples of the opposite relations can also be cited. For instance, in models ZLW1-1 (Fig. 84) or ZLW1-3 (Fig. 87), Zn predominates in the vein, and Pb has the most intense maximum in the aureole (A-type distribution).

Other situations were also examined in our simulations. In model ZRW1-1 (Fig. 88), the vein is practically devoid of ore minerals (because of the reaction mechanism that produced the vein), but the neighboring aureole shows high concentrations of Zn and Pb. Situations of this type were encountered in natural environments, as exemplified by profiles 5 and 7 near the Vertikal'naya Vein (Kholst, level VII). The vein (ore suture) itself has Pb and Zn concentrations on the order of 0.0n%, while the concentrations of these elements in the aureole are one order of magnitude higher.

(6) Most of our models yield realistic proportions of minerals in the altered wall rocks. For example, models ZRW1-3 and ZLW1-3 exhibit the development of quartz–sericite with chlorite metasomatic assemblages, which are analogous to the assemblages ubiquitous at the deposits and have the same proportions of the main minerals (up to 60% quartz and up to 30% sericite, Fig. 87). However, wall-rock K-feldspathization near the vein obtained in some models at high temperatures (models ZRW1-1 and ZRW4-1, Fig. 97) is generally atypical of the deposits. Conceivably, this may suggest that more realistic simulation results were yielded by models with equally high temperatures but with reactors that imitate the development of an aureole containing not 100, but 10 g, of rock. In this situation, the altered wall rocks have a normal quartz–muscovite–chlorite composition (Fig. 91). It is quite probable that this result provides independent evidence that the reactors adjacent to the vein should have lower rock/water ratios than those in more distant reactors. This tendency in the variations of the rock/water ratio was mentioned above, where the modeling methods in the zone of aureole formation were discussed (Section 6.3.1, Fig. 81).

(7) We devised only one model for leaching aureoles, because the processes occurring in these zones were closely examined in the section devoted to the mobilization zone of ore components (Section 6.1). The results of model FM1 are in good agreement with geochemical data on the deposits: the wall-rock alterations near the orebodies are at a minimum (Fig. 99), and weak positive (up to 2–3 clarkes) and negative anomalies of ore elements can be formed near the vein (this is typical of Zn, compare Figs. 98 and 46).

6.3.4. Conclusions

The models for the development of aureoles led us to the following conclusions:

(1) The structure proposed for the models and the techniques devised for simulating the origin and evolution of ore-element aureoles in wall rocks around veins at base-metal deposits involves a complex of interrelated events over the interval of the mobilization zone to the zone where orebodies and aureoles are formed.

(2) Our simulations indicate that a temperature gradient and chemical interactions in the solution-rock system are the main factors controlling the behavior of ore material in the aureole.

(3) The models allowed us to obtain all principal types of aureoles typical of the deposits in question: aureoles of deposition, redeposition, and leaching. The possible conditions, causes, and mechanisms of their formation are analyzed.

(4) It is demonstrated that equilibrium-dynamic modeling makes it possible to assay the main tendencies in the development of aureoles and the main parameters that predetermine their distinctive features.

6.4. General Conclusions on Chapter 6

At the end of each section of this chapter, we presented the results and main conclusions. Below is a general review.

(1) A generalized structure and methods were worked out for the equilibrium-dynamic simulation of the processes producing vein base-metal ore mineralization over the interval from the mobilization zones of the metals to the zones where orebodies develop and aureoles of ore elements in the wall rocks are formed. This basis was used to devise a generalized quantitative model for an ore-forming hydrothermal system for vein base-metal deposits.

(2) The models indicate that the rock-water interaction is the most important factor that controls the genesis of hydrothermal ores and whose action is discernible during each evolutionary stage of the hydrothermal system. This is the main process forming mineralized solutions in the mobilization zone. In the zone of ore formation these are the processes of intraore metasomatism and in the zone of aureoles the main factor that controls their development.

(3) When a barren solution interacts with granite, a mineralized metalliferous solution is produced, whose concentrations of ore elements significantly increase with time even without any changes in the external conditions and then decrease upon the complete depletion of some elements from the source granite in the mobilization zone of the metals. The metalliferous potential of the leaching solution varies in the course of the mobilization processes.

(4) Our modeling results confirm that the development of orebodies without redeposition is the main mechanism generating ore mineralization, while intraore metasomatism plays a subordinate role, although the latter processes are widespread. Stages of

mineral formation can be explained from the viewpoint of the continuous evolution of a single source of the ore material (in our models, this is the host granite).

(5) Temperature gradients and interactions in the solution-rock system are the main factors controlling the deposition of ore material in the aureole. Our models yield three main types of aureoles typical of the deposits in question: aureoles of deposition, redeposition, and leaching.

(6) Our model describes the spatiotemporal evolution of the hydrothermal system, its principal structural features, and the main regularities in the distributions of elements in vein bodies and aureoles. The results accurately reproduce the quantitative and qualitative characteristics of natural mineral associations.

SUMMARY

Our research is an attempt to reconstruct the processes that controlled the origin and evolution of orebodies and associated primary aureoles of metals at hydrothermal vein deposits based on the further development of methods currently utilized in geochemical studies and thermodynamic simulation. Although we proceeded from a few mineral deposits, our models led us to conclusions that are more general and applicable to a wide circle of deposits, in spite of the discouraging remark made by H.P. Taylor, Jr., that any mineral deposit seems to be a unique phenomenon, and this makes it difficult to expand the results of investigations devoted to the nature and evolution of the hydrothermal metalliferous fluid or fluids, which is especially true in relation to most hydrothermal vein deposits [*Geochemistry of Hydrothermal Ore Deposits*, 1979].

We explored models for the genesis of ore mineralization that were characterized by progressively more complicated physicochemical parameters of the ore-forming systems in the following succession:

- * a model of U mineralization in rocks with heterogeneous filtration characteristics but a uniform chemical composition and constant temperature and pressure (the prototype of this model is the Chauli deposit);

- * a model of U mineralization hosted by rocks with contrastingly different chemical compositions but with constant temperature and pressure (deposits of the unconformity type);

- * a model of vein base-metal mineralization formed under gradients of temperature and pressure in chemically homogeneous rocks (deposits of the Sadon group).

The main conclusions can be summarized as follows.

It was established for all models that *the source of the ore components can be rocks that host the deposit or contained in the local geologic sequence*. It is also important that *the formation of a deposit does not require that the source rocks contain more than clarke concentrations of the ore elements*.

The sources can be different for different components. At uranium deposits, the sources of the metals and precipitator components are different: the precipitants (sulfide sulfur or methane) are mobilized when the solutions react with rocks under reduced conditions (graphite- and pyrite-bearing schists), while the metals are extracted from rocks of normal granitoid composition under more oxidized conditions. The large drainage areas (and, hence, great volumes of the recycled rocks from which the metals are extracted) usually predetermine significant or giant reserves of these deposits (this applies, first and foremost, to unconformity-type deposits and large vein-type deposits).

The base-metal deposits discussed in this publication most probably had the same sources of the metals and sulfide sulfur: this was the Sadon granite, which was low in sulfide sulfur. The ore components were mobilized from restricted areas, and, as a consequence, the deposits have intermediate or even small reserves.

Ores were formed in all of our models without variations in the external conditions.

In our models for the genesis of U mineralization, the temperature, pressure, and the compositions of the primary barren and metalliferous solutions remain constant. The main cause of ore precipitation is the mixing of hydrothermal solutions either at *stationary* hydrodynamic geochemical barriers, which are determined by the heterogeneity of the filtration characteristics of the host geological environment (as at the Chauli deposit), or at *mobile* geochemical barriers of hydrodynamic nature, which are created by flows of filtrating solution from "black schists" (as at unconformity-type deposits). Changes in the filtrations regime of the flows of the metalliferous solution and the "precipitant" solution result in the formation of various mineral assemblages, up to monomineralic orebodies.

In the genetic model for base-metal ore mineralization, the composition of the primary "barren" solution also does not vary throughout all mineral "stages," and the vertical temperature gradient can also remain constant. The main causes of ore precipitation, which control the variations in the composition of the filling veins with time, are *the compositional evolution of the metalliferous hydrothermal solution in the zone where the ore components are mobilized and the temperature decrease in the fracture-vein systems.*

The models demonstrate that the spatially uneven development of vein and wall-rock mineral assemblages, including their separation in space and rhythmical alternations, are the natural consequences of the hydrodynamic conditions under which the vein ores are formed (as is exemplified by the Chauli deposit). Thus, the scarcity of wall-rock alterations near fractures or, more often, even their absence cannot be regarded as evidence of the absence of active material exchange between the wall rocks and solution in the fracture. This material exchange is mediated not by the rocks but by the pore solution in equilibrium with them.

In this context, it is pertinent to recall G.L. Pospelov's [1963] comment that "...it is reasonable to believe that the formation of a deposit requires such a combination of conditions that is less probable than the existence of potentially efficient metalliferous hydrothermal solutions that are able to precipitate ore mineralization." At least, our models with the active action of hydrothermal barriers justify this statement.

GENERAL CONCLUSIONS

(1) We elaborated new methods for assaying the composition of hydrothermal solutions based on the results of simulations of metasomatic alterations in rocks exerted by rock-solution reactions. The study of interactions in the rock-water system makes it possible to predict geochemical phenomena in naturally occurring systems of rocks and thermal waters. The interaction of barren solutions with granitoids gives rise to metalliferous solutions that can be parental for the hydrothermal systems in question. The metalliferous potential of these solutions is significantly enhanced in the course of the mobilization process because of the progressive leaching of sulfide sulfur from the rocks without any variations in the external conditions.

(2) The self-mixing mechanism is able to maintain conditions necessary for the formation of ores from metals disseminated in the country rocks: extraction of ore elements from large volumes of rocks, migration of the metals extracted by the solutions into the local volumes of fracture conduits, and the concentrated (sometimes selective) precipitation of the metals at hydrodynamic geochemical barriers. This process can proceed under constant P , T conditions and without any variations in the composition of the barren solution that comes into the hydrothermal system. A natural consequence of the process is the spatial separation of syngenetic metasomatic rocks and ores.

(3) The interaction of the solutions with graphite- and pyrite-bearing rocks results in flows of barren reducing solutions with dissolved hydrogen sulfide and methane. When these solutions mix with metalliferous solutions equilibrated with granitic rocks, mineralized veins or unconformity-type deposits can be formed in crosscutting fractures or regional unconformity zones. Changes in the filtration regimes and mixing proportions of the solutions (at unchanging other conditions) are an efficient mechanism that brings about systematic variations in the mineral assemblages of the orebodies. Hydrothermal solutions of this type can produce rich ores practically devoid of gangue minerals.

(4) The first data were obtained on the fine distribution structures of ore elements in wall rocks around veins at hydrothermal deposits of the vein base-metal type. It is demonstrated that detailed structures of the aureoles can be used as the basis for models of the genesis of aureoles and ores. The aureoles are classified